



# The effect of oxygen-free $\text{MgF}_2$ matrix on the physical properties of $(\text{CoFeZr})_x(\text{MgF}_2)_{100-x}$ nanocomposites

O. V. Stognei, T. V. Tregubova<sup>†</sup>, I. M. Tregubov

<sup>†</sup>ttv1507@ya.ru

Voronezh State Technical University, Voronezh, 394006, Russia

Structure, electrical, magnetic and magnetoresistive properties of  $(\text{CoFeZr})_x(\text{MgF}_2)_{100-x}$  thin film composites have been investigated in a wide range of metal phase concentration ( $14 \text{ at.}\% \leq x \leq 52 \text{ at.}\%$ ). The composites were studied in the initial state and after heat treatment at different temperatures up to  $350^\circ\text{C}$ . The magnetoresistance of the samples in initial state reached 3.25% in a magnetic field of 10 kOe. It was established that the composites magnetoresistance and magnetic properties are steady against thermal heating up to  $350^\circ\text{C}$ . It is assumed that the stability of the composites properties against annealing is due to the presence of zirconium atoms dissolved in the dielectric matrix.

**Keywords:** thin films, magnetoresistance, electric properties, structure, thermal stability.

## 1. Introduction

The nanogranular metal - dielectric composites are two-phase heterogeneous systems where dimension of the phases inclusions do not exceed several nanometers. The most attractive for the practical application are pre-percolated composites where metal nanogranules are separated from each-others and randomly distributed in a dielectric matrix. One of the most characteristic properties of the pre-percolated ferromagnetic metal - insulator composites is a tunnel magnetoresistance (TMR). The relatively high values of TMR are usually observed in the cobalt-based composites [1–8]. For example, the TMR value is 7–8% in composites with mono-element ferromagnetic phase (Co-Al-O [2,7]). In order to improve physical properties of the composites ferromagnetic alloys are used instead of pure metal. The TMR values in CoFe alloy-based composites are larger (10–12%) than in composites with pure cobalt granules [1, 3, 5, 6]. On the other hand, the cobalt-based composites are perspective as a material for high-frequency applications in inductors, generators, sensors, transformers and others [9,12]. Such materials has to be soft magnetic and in order to achieve required properties in Co-based nanocomposites one should reduce the strong crystallographic anisotropy of metal granules. The obvious way to achieve that is application of an amorphous ferromagnetic alloy and the nanocomposites with CoFeZr metal phase are good candidate for such purpose [9–12]. The amorphous structure of the alloy is due to presence of the Zr atoms [10] and mutual vacuum deposition of this alloy and aluminum oxide provides the formation of the composite structure were both metal and dielectric have amorphous structure [9–12]. The metal granules in the CoFeZr-based composites with oxide dielectric matrix are oxidized and it has been established that the granules are core-shell particles where the “shell” is a Co or Fe oxide [11,12]. It is negative for some application

therefore the oxygen-free dielectric matrix (for example metal fluorides  $\text{MgF}_2$  or  $\text{AlF}_3$ ) can be used to avoid oxidation of the composites metal phase [3–6,8]. Within such approach the investigation of the new Co-based composites with oxygen-free fluoride matrix has been carried in the present work.

The composites formed from CoFeZr ferromagnetic nanoparticles and non-oxide  $\text{MgF}_2$  matrix have been obtained in a wide range of the phase's ratio. The influence of the non-oxide  $\text{MgF}_2$  matrix on the electrical and magnetoresistive properties as well as on the thermal stability of the  $(\text{CoFeZr})_x(\text{MgF}_2)_{100-x}$  nanocomposites has been studied.

## 2. Materials and experimental methods

The ion-beam sputtering of a mosaic target in argon atmosphere was used to obtain the composite samples. The target was made from metal ( $\text{Co}_{47}\text{Fe}_{42}\text{Zr}_{11}$ ) base with several  $\text{MgF}_2$  dielectric plates on its surface. The  $\text{MgF}_2$  plates were attached unevenly on the target surface and that gave the possibility to obtain samples with different concentration of the metal phase in one technological cycle. Sputtered atoms of the metal and dielectric materials were simultaneously deposited on substrates and formation of a composite structure (that is a separation onto metal and dielectric phases) was being occurred in the depositing film due to a self-organizing process. Two types of substrates were used: sital (glassceramic) for magnetic and resistive measurements and glass — for X-ray diffraction.

The concentration of chemical elements in the composites was measured by electron-beam probe X-ray spectral microanalysis JXA-840t. It has been determined that concentration of the metal phase in the obtained samples gradually changes from 14 to 52 at.%. The phase composition was determined by X-ray diffraction (XRD) at BRUKER D2 Phaser diffractometer in a Bragg-Brentano geometry. The

resistance measurements of the samples were carried out by the two-probe potentiometric method. The possibility of using the two-probe method was due to the high resistivity of the studied samples. The magnetoresistance was investigated by direct measurements of the samples electrical resistance when the external magnetic field was being changed from 0 to 10 kOe. Investigation of the composites magnetic properties was carried out by vibrating sample magnetometer. The thickness of the obtained samples was measured by Linnik interferometer. It has been determined that the samples thickness is varied within 1–3  $\mu\text{m}$  depending on the metal concentration.

### 3. Results and discussion

Preliminary it was assumed that the metal phase of the forming  $(\text{CoFeZr})_x(\text{MgF}_2)_{100-x}$  composites should be amorphous. This assumption was based on the presence of zirconium atoms in the metal phase. It is known that zirconium acts as an amorphizer in the metal CoFe alloys and it is possible to obtain an amorphous or a crystalline structure just by varying the zirconium concentration [9–11]. However, XRD analysis has showed that both formed phases of the composites are crystalline (Fig. 1). The metal phase has crystalline structure of bcc CoFe alloy and the dielectric phase has structure of magnesium fluoride  $\text{MgF}_2$ . Moreover, two structure modifications of the magnesium fluoride (P42/mnm and P4/nmm) were determined in the  $(\text{CoFeZr})_{38}(\text{MgF}_2)_{62}$  composite (Table 1). There are peaks from both modifications on the XRD curve from the mentioned sample (Fig. 1). Formation of the crystalline metal phase in the  $(\text{CoFeZr})_x(\text{MgF}_2)_{100-x}$  composite is quite untrivial result. The CoFeZr metal alloy is often used to prepare metal-dielectric composites with soft magnetic properties ( $\text{CoFeZr-SiO}_2$ ,  $\text{CoFeZr-Al}_2\text{O}_3$ ) [9–12, 21–23] and structure of the metal phase was amorphous in all cases when dielectric phase was an oxide.

Based on the obtained data one can assume that the Zr atoms are not included into the CoFe metal alloy during the deposition process. Instead of this the zirconium is being dissolved in the the magnesium fluoride. This assumption is confirmed by the fact that formation of a chemical bonds between zirconium and fluorine is energetically advantageous: the Gibbs energy of  $\text{ZrF}_4$  formation is quite large ( $\Delta G_{\text{ZrF}_4} = -1809$  kJ/mol) [13]. The CoFe metal alloy without the amorphizer (under conditions of lack of Zr atoms) is being formed with crystalline structure. In its turn the zirconium atoms dissolved in the  $\text{MgF}_2$  form regions with the distorted  $\text{MgF}_2$  lattice which give the diffraction peak (220) on the XRD curve (Fig. 1).

Concentration dependence of the  $(\text{CoFeZr})_x(\text{MgF}_2)_{100-x}$  composites resistivity is typical for classic metal-dielectric

nanocomposites (Fig. 2). It can be divided into three areas: pre-threshold, post-threshold and percolation threshold itself. In metal-dielectric nanocomposites electrical percolation threshold is a metal phase concentration where formation of a percolation cluster occurs [7, 14–16]. The metal concentration in a composite reaches so large value that separated metallic granules is being joined to conducting chains. In other words it is a concentration where charge transfer mechanism is changed from non-metallic to a metal one. The conductivity of such transition media depends on metal concentration very much. Small changes in the composition lead to a significant (by several orders of magnitude) change in the sample resistance. Therefore, the percolation threshold corresponds to the middle of the concentration interval where the sharp resistance decreasing occurs. The correctness of determining the position of the percolation threshold is also confirmed by the temperature dependences of samples resistance,

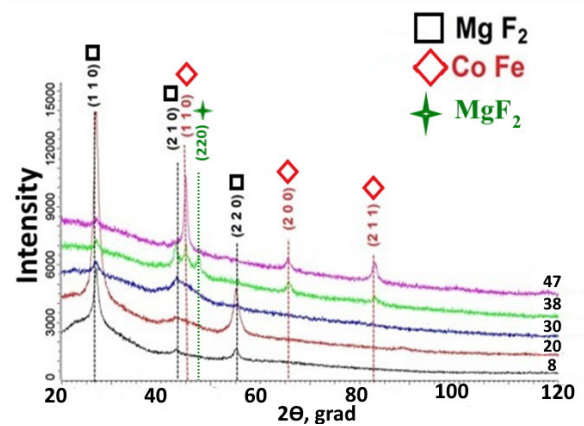


**Fig. 1.** (Color online) XRD of  $(\text{CoFeZr})_x(\text{MgF}_2)_{100-x}$  samples with different concentrations of the metal phase. The concentration of the metal phase (in at. %) is indicated by numbers on the curves.

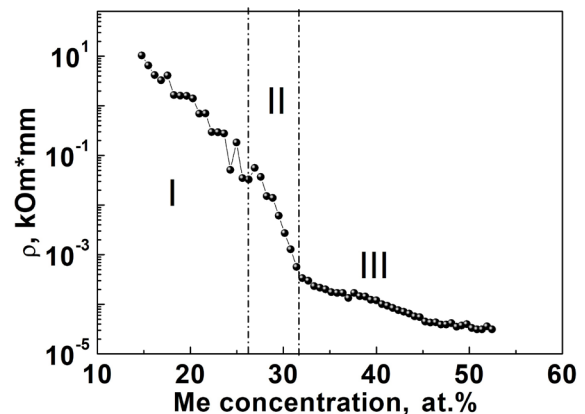


**Fig. 2.** Concentration dependence of electrical resistivity of  $(\text{CoFeZr})_x(\text{MgF}_2)_{100-x}$  composites.

**Table 1.** Lattice parameters of the  $\text{MgF}_2$  phases observed in the  $(\text{CoFeZr})_{38}(\text{MgF}_2)_{62}$  composite.

	(hkl)	2θ, grad	The lattice type	a, Å	c, Å	Volume, Å <sup>3</sup>	Crystallographic orientation
$\text{MgF}_2$	(110)	27	Tetragonal	4.69	3.096	68	P42/mnm
	(210)	43					
	(220)	56					
$\text{MgF}_2$	(220)	48	Tetragonal	4.06	3.82	63	P4/nmm

as well as the TMR values (see below). In the studied  $(\text{CoFeZr})_x(\text{MgF}_2)_{100-x}$  system the electrical percolation threshold, determined on a base of the concentration dependence (Fig. 2), takes place at 27 at.% of the metal phase. This value is much smaller than the threshold position in known oxide systems such as  $\text{Co-SiO}_2$ ,  $\text{Co-Al}_2\text{O}_3$ ,  $\text{CoFeB-SiO}_2$ ,  $\text{CoFeZr-Al}_2\text{O}_3$ ,  $\text{CoNbTa-SiO}_2$  and others [7, 14–16, 21]. In other words the threshold position in the  $(\text{CoFeZr})_x(\text{MgF}_2)_{100-x}$  system is shifted to a dielectric region compared to the composites with oxide dielectric phases, where the threshold position is 40–60 at.% Me. Such result is probably a consequence of the features of a fluoride dielectric matrix. Much less metal phase is needed for formation of a percolation cluster, since the metal is not oxidized and the granules are not covered by an oxide shell that prevents the formation of the percolation cluster.

Tunnel magnetoresistance was detected in all  $(\text{CoFeZr})_x(\text{MgF}_2)_{100-x}$  composite samples with concentration of the metal phase corresponding to regions I and II (below and on the percolation threshold, Fig. 3). It should be noted that only negative magnetoresistance was detected in the  $(\text{CoFeZr})_x(\text{MgF}_2)_{100-x}$  composites: the resistance of the samples decreases with an increase of the magnetic field. The TMR values depend radically on the concentration of the metal phase. Maximum TMR value corresponds to the concentration of the metal phase in the vicinity of the percolation threshold where the width of the dielectric barrier between neighbor granules is minimal but magnetic interaction between granules is still absent (Fig. 4). Such morphology is optimal for direct electron tunneling between granules that provides maximum tunnel current under external magnetic field which corresponds to the maximum magnetoresistive effect.

The measured maximum values of the TMR (3.25%) are comparable to the TMR values obtained in the oxide matrix composites (for example, the TMR value does not exceed 3.8% in  $(\text{Co}_{45}\text{Fe}_{45}\text{Zr}_{10})_x(\text{SiO}_2)_{100-x}$  composites [17, 21]). In other words the non-oxide dielectric matrix as well as crystalline structure of the metal nanogranules do not give significant changes into the magnetoresistive effect. It is quite understandable because the TMR is due to tunneling of spin-polarized electrons through the dielectric barriers between

ferromagnetic (superparamagnetic) granules. The TMR value mainly depends on geometry (the distance between granules which is always optimal in the vicinity of the percolation threshold) and electron polarization coefficient of metal phase which does not depends on its structure (crystalline or amorphous) [24, 25].

Heat treatment of the composite samples whose composition corresponds to the percolating threshold (26–30 at.% of the metal phase) leads to significant decrease of the TMR values (Fig. 4). This known effect is due to increasing of average nanogranules size occurring during the heat treatment [18–20]. The percolating cluster can be formed during the treatment because initial distance between granules in the composites which are on the threshold was minimal.

That is why the TMR in composites with 29 at.% of metal decreases almost to zero after annealing. On the other hand the thermal stability of the magnetoresistive effect is high in the  $(\text{CoFeZr})_x(\text{MgF}_2)_{100-x}$  composites from the pre-percolating region and only insignificant decrease of TMR values was observed (Fig. 4). The high thermal stability of the TMR values is hardly determined by the composition of the dielectric matrix. One should note that thermal stability of magnetoresistance in similar composite system with the same matrix ( $\text{Co-MgF}_2$  composites) is much smaller. It has been shown that magnetoresistance disappears in pre-percolating  $\text{Co-MgF}_2$  samples after heat treatment at 350°C [8].

It is known that an electrical resistance is a structure-sensitive characteristic of condensed matters. Therefore the temperature dependence of the composites electrical resistance was investigated in order to establish a temperature of possible phase transitions. The obtained dependences are characteristic for metal-dielectric composites [5, 15, 16]. Three typical dependencies obtained for  $(\text{CoFeZr})_x(\text{MgF}_2)_{100-x}$  composites from three different regions of  $\rho$  vs  $x$  dependence (Fig. 2) are shown on the Fig. 5. There is a wide resistance maximum in temperature region upper 200°C in the pre-percolation composites (curve 1, Fig. 5), there is a resistance decrease with temperature rising in samples which are below the percolation threshold (curve 3, Fig. 5) and samples located on the percolating threshold show combined temperature dependence.

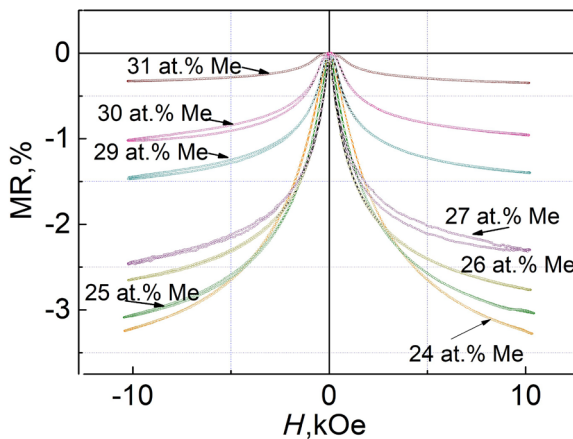


**Fig. 3.** (Color online) Field dependences of  $(\text{CoFeZr})_x(\text{MgF}_2)_{100-x}$  composites magnetoresistance with different concentrations of the metal phase.

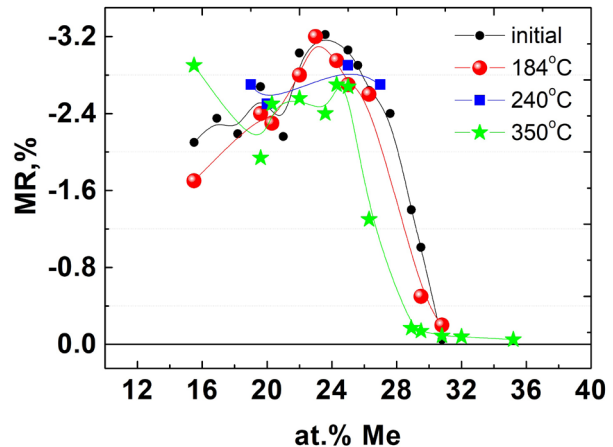


**Fig. 4.** (Color online) Concentration dependence of the  $(\text{CoFeZr})_x(\text{MgF}_2)_{100-x}$  composites magnetoresistance in initial state and after annealing.

The increase of the resistance in the pre-percolation composites (15–25 at.% of the metal phase) is associated with the relaxation processes occurring in the dielectric matrix during annealing. The morphology of these composites is a separated from each-other metal nanogranules randomly distributed in a dielectric matrix therefore the tunnel conductivity is realized in these samples. The electrons can tunnel directly from granule to granule so it brings the TMR effect. They can also tunnel via localized states (structural defects in the dielectric), this mechanism is called “hopping conductivity”, and it does not depend on the magnetic field. In any cases these composites do not content percolating clusters therefore their resistivity is high. The heat treatment stimulates relaxation processes including diffusion of metal atoms, dissolved in the matrix, towards the granules. These processes reduce the number of structural defects in the dielectric and leads to reduction of the hopping conductivity that increases the resistance [15,16], curve 1 on Fig. 5. At the same time these processes do not give the formation of the percolating clusters because original distances between granules are quite large hence the possible increasing of the granules size due annealing does not lead to their coalescence. The preservation of an electrically uncoupled medium (the granules are still separated in the volume of the dielectric) determines a high resistance of the samples. On the other hand it explains why the TMR in the pre-percolated samples is not changed after heat treatment at 184°C, 240°C and 350°C (see Fig. 4). In other word one can assume that until the sample resistance is being monotonically increasing during the heating the granular non-coalesced structure is preserved. The resistance maximum is observed at upper temperatures (in temperature interval of 350–450°C, depending on the metal concentration), therefore, the heat treatment of the samples at 350°C (it was made for TMR investigation) does not bring structure transformation to the composites.

If the initial distance between granules is small (the percolation region, 26–30 at.% of the metal phase) the heat treatment leads to percolating cluster formation and instead of rising of the samples resistance it's decreasing is observed

in a temperature interval of 200–350°C (curve 2, Fig. 5). The clusters formation changes the conductivity mechanism in the composites from tunneling to metallic one and as a consequence the TMR is practically disappeared (see Fig. 4).

The resistance of the composites which are below the percolation threshold ( $30 < x$ , at.%) decreases with temperature rising (curve 3, Fig. 5). These composites have inverse morphology: the metal phase is a continuum matrix and the dielectric forms a discreet phase. Even close to the percolation threshold the composites have conductivity clusters. The resistance decreasing is due to recrystallization of the metal phase. This process reduces the degree of defectiveness of the conductive medium, at least the density of grain boundaries decreases as a result of the recrystallization.

Analysis of the XRD data of the samples in the initial state and after annealing suggests an increase of the average size of CoFe metal nanogranules as a result of the heat treatment (Fig. 6). The granules increase during a heat treatment was observed in different composite systems [18–20]. Considering the fact that the grain growth occurs due to the diffusion of metal atoms, dissolved in the dielectric matrix, it is reasonable to suggest that the increase of the granules size would provide the magnetic interaction between them. The interaction would lead to the formation of magnetic macrodomains and, as a consequence, macroscopic ferromagnetic properties should be observed in annealed composites. The macrodomains can be formed even in samples witch are before the percolation threshold when electrical percolation has not yet occurred. The presence of the macrodomains should depress the TMR because magnetic ordering of the granules moments will take place within the domains. In this case the mutual orientation of the granules magnetic moments will not depend on the presence or absent of external magnetic field. However, TMR remains in the  $(\text{CoFeZr})_x(\text{MgF}_2)_{100-x}$  nanocomposites from the pre-percolation region after their annealing at 350°C.

Investigation of the composites magnetic properties in the initial state and after annealing at 350°C showed that heat treatment practically does not affect the

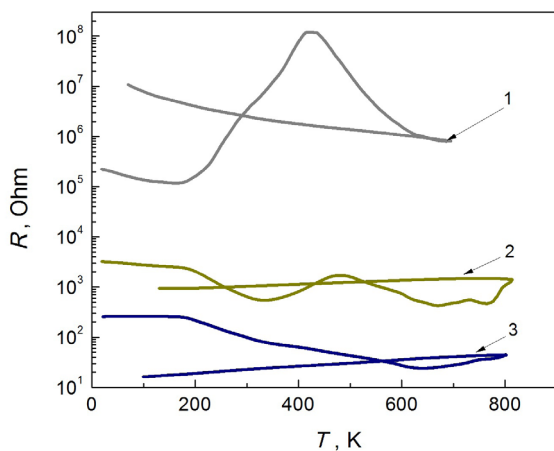


**Fig. 5.** (Color online) Temperature dependence of the electrical resistance of  $(\text{CoFeZr})_x(\text{MgF}_2)_{100-x}$  nanocomposites with different concentration of the metal phase and located at different position relatively the percolation threshold. 1 —  $x=13$  at.% (pre-percolated sample); 2 —  $x=30$  at.% (sample on the percolation threshold); 3 —  $x=33$  at.% (sample below the threshold).

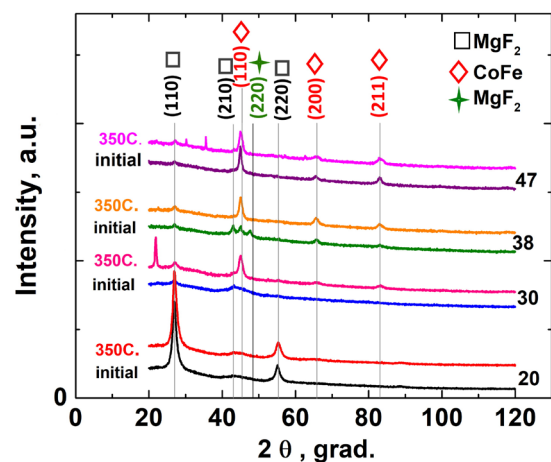


**Fig. 6.** (Color online) XRD of  $(\text{CoFeZr})_x(\text{MgF}_2)_{100-x}$  samples in the initial state and after annealing at  $T=350^\circ\text{C}$  with different concentrations of the metal phase. The concentration of the metal phase (at.%) is indicated by numbers.



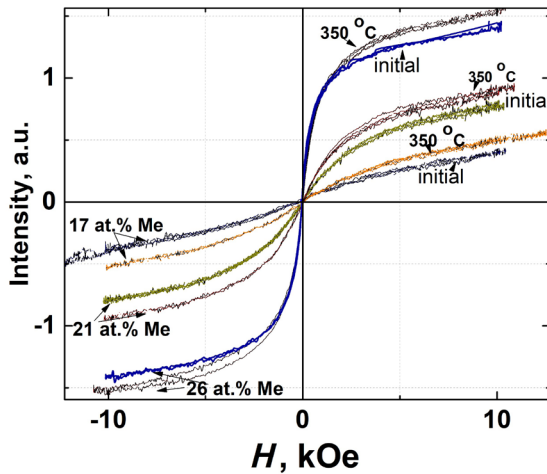


**Fig. 7.** (Color online) Field dependences of magnetization of the  $(\text{CoFeZr})_x(\text{MgF}_2)_{100-x}$  composites in the initial state and after annealing at  $350^\circ\text{C}$ .

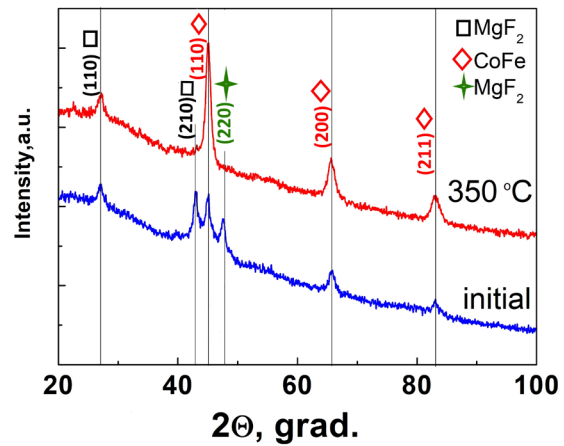


**Fig. 8.** (Color online) XRD of the  $(\text{CoFeZr})_{38}(\text{MgF}_2)_{62}$  sample in the initial state and after annealing at  $T = 350^\circ\text{C}$ .

magnetic characteristics of the composites — the same superparamagnetic characteristics were observed in the samples after annealing as well as in the initial state (Fig. 7). It means that no ferromagnetic regions were formed during annealing. We believe that the thermal stability of the TMR effect in the  $(\text{CoFeZr})_x(\text{MgF}_2)_{100-x}$  composites is due to the presence of dissolved zirconium atoms in the dielectric phase and diffusion of these atoms caused by heat treatment. During the annealing process the diffusing zirconium atoms reach the interfacial boundary (the surface of metal granules) and form a paramagnetic shell (zirconium is a paramagnetic material). From one hand the shell increases the size of the granules (it follows from the XRD data) but on the other hand it does not help the ordering of the granules magnetic moments and, consequently, prevents the forming of macroscopic ferromagnetism (it does not observed experimentally, Fig. 7).

This assumption is confirmed by the XRD data of the  $(\text{CoFeZr})_{38}(\text{MgF}_2)_{62}$  sample annealed at  $350^\circ\text{C}$  (Fig. 8). The peak (220) at  $2\theta = 48^\circ$  corresponding to the reflection from the  $\text{MgF}_2$  with distorted lattice due to dissolved Zr atoms, disappears after annealing. One can explain this result as a diffusion of zirconium atoms from dielectric volume to the interphase boundaries.

#### 4. Conclusions

Nanocomposite  $(\text{CoFeZr})_x(\text{MgF}_2)_{100-x}$  samples have been obtained by the vacuum deposition technique. Both (metal and dielectric) phases of the obtained composites are crystalline. It is assumed that zirconium atoms are dissolved in the  $\text{MgF}_2$  dielectric phase during the formation of the composites.

The  $(\text{CoFeZr})_x(\text{MgF}_2)_{100-x}$  composites in the pre-percolating region exhibit a giant magnetoresistive effect that reaches 3.25% in the vicinity of the percolating threshold. These TMR values are comparable with the values observed in metal-oxide composites.

It has been established that the presence of an oxygen-free dielectric matrix significantly shifts the electrical percolation threshold in  $(\text{CoFeZr})_x(\text{MgF}_2)_{100-x}$  composites to the dielectric

region (down to 27 at.% of the metal phase) compared to composites based on oxide matrixes (40–50 at.% metal phase).

The  $(\text{CoFeZr})_x(\text{MgF}_2)_{100-x}$  composites with metal phase concentration lower the percolating threshold exhibit stability to the heat treatment. Both the magnetoresistive effect as well as the superparamagnetic properties of the composites are not being changed under vacuum heat treatment at the temperature up to  $350^\circ\text{C}$ .

*Acknowledgements.* This research was funded by the Ministry of Science and Higher Education of the Russian Federation, project FZGM-2023-0006 and the contract 075-15-2021-709, unique identifier of the project RF-2296.61321X0037 (equipment maintenance).

#### References

1. S. Kanie, S. Koyama. Aip Adv. 8, 056313 (2018). [Crossref](#)
2. N. Kobayashi, S. Ohnuma. JMMM. 188, 30 (1998). [Crossref](#)
3. N. Kobayashi, S. Ohnuma. J. Appl. Phys. 90, 4159 (2001). [Crossref](#)
4. Y. Cao, A. Umetsu, N. Kobayashi. Appl. Phys. Lett. 111 (12), 122901 (2017). [Crossref](#)
5. S. Koyama, J. Totsuka. J. Appl. Phys. 113, 17C720 (2013). [Crossref](#)
6. N. Kobayashi, S. Ohnuma, H. Fujimori. J. Jpn. Inst. Met. 76, 375 (2012). (in Japanese). [Crossref](#)
7. S. Mitani, H. Fujimori. JMMM. 177, 919 (1998). [Crossref](#)
8. T. V. Tregubova, O. V. Stognei, V. V. Kirpan, A. V. Sitnikov. EPJ Web of Conf.: MISIM. 185, 01014 (2018). [Crossref](#)
9. J. Fedotova et al. 9th IEEE Conf. on Nanotech. (IEEE-NANO), (2009) p. 651.
10. J.-O. Song, S.-R. Lee. JMMM. 310, 1923 (2007). [Crossref](#)
11. J. A. Fedotova, A. V. Pashkevich et al. JMMM. 511, 166963 (2020). [Crossref](#)
12. T. N. Koltunowicz et al. JMMM. 421, 98 (2017). [Crossref](#)
13. V. A. Rabinoviich. Brief Chemical Reference. V. II. Leningrad, Khimiya (1978) 392 p. (in Russian)

14. S. Sankar, A.E. Berkowitz, D.J. Smith. Phys.Rev. B. 62 (21), 14273 (2000). [Crossref](#)
15. Yu. E. Kalinin, A. V. Sitnikov, O. V. Stognei. Alt. Ener. and Ecol. 10, 9 (2007).
16. O. V. Stognei, V. A. Slyusarev. Microelectr. Eng. 69 (2-4), 476 (2003). [Crossref](#)
17. A. V. Shchekochihin et al. Kondensirovannye sredy i mezhfaznye granicy. 11 (1), 78 (2009). (in Russian)
18. J.-G. Ha, S. Mitani, K. Takanashi, M. Ohnuma. JMMM. 198, 21 (1999). [Crossref](#)
19. M. Ohnuma, K. Hono, H. Onodera et al. NanoStruct. Mater. 12, 573 (1999). [Crossref](#)
20. B. Dieny, S. Sankar, M.R. McCartney et al. JMMM. 185, 283 (1998). [Crossref](#)
21. A. Granovsky, Yu. Kalinin, O. Stognei et al. Physics Procedia. 82, 46 (2016). [Crossref](#)
22. A. M. Saad et al. Rev. Adv. Mater. Sci. 8, 152 (2004).
23. I. A. Svito et al. J. Alloys. Comp. 699, 818 (2017). [Crossref](#)
24. M. Julliere. Phys. Lett. 54A (3), 225 (1975). [Crossref](#)
25. J. S. Moodera, L. R. Kinder, et al. Phys. Rev. Lett. 74, 3273 (1995). [Crossref](#)